

# Disentangled Partial Label Learning

Wei-Xuan Bao<sup>1, 2</sup>, Yong Rui<sup>3</sup>, Min-Ling Zhang<sup>1, 2\*</sup>

<sup>1</sup>School of Computer Science and Engineering, Southeast University, Nanjing, China

<sup>2</sup>Key Laboratory of Computer Network and Information Integration (Southeast University), Ministry of Education, China

<sup>3</sup>Lenovo Research, Lenovo Group Ltd., Beijing, China

baowx@seu.edu.cn, yongrui@lenovo.com, zhangml@seu.edu.cn

## Abstract

Partial label learning (PLL) induces a multi-class classifier from training examples each associated with a set of candidate labels, among which only one is valid. The formation of real-world data typically arises from heterogeneous entanglement of series latent explanatory factors, which are considered intrinsic properties for discriminating between different patterns. Though learning disentangled representation is expected to facilitate label disambiguation for partial-label (PL) examples, few existing works were dedicated to addressing this issue. In this paper, we make the first attempt towards disentangled PLL and propose a novel approach named TERIAL, which makes predictions according to derived disentangled representation of instances and label embeddings. The TERIAL approach formulates the PL examples as an undirected bipartite graph where instances are only connected with their candidate labels, and employs a tailored neighborhood routing mechanism to yield disentangled representation of nodes in the graph. Specifically, the proposed routing mechanism progressively infers the explanatory factors that contribute to the edge between adjacent nodes and augments the representation of the central node with factor-aware embedding information propagated from specific neighbors simultaneously via iteratively analyzing the promising subspace clusters formed by the node and its neighbors. The estimated labeling confidence matrix is also introduced to accommodate unreliable links owing to the inherent ambiguity of PLL. Moreover, we theoretically prove that the neighborhood routing mechanism will converge to the point estimate that maximizes the marginal likelihood of observed PL training examples. Comprehensive experiments over various datasets demonstrate that our approach outperforms the state-of-the-art counterparts.

## Introduction

Data-driven deep learning (LeCun, Bengio, and Hinton 2015) has achieved remarkable success in numerous application scenarios. Its superiority could be primarily attributed to the accessibility of vast amount of supervised training data. Nevertheless, constrained by expertise and efforts, extensive data annotation could inevitably induce ambiguity and label noise, which might impose detrimental effects on

model training (Wei et al. 2022; Hu et al. 2022; Yang, Liu, and Yin 2022). It is desirable to explore endowing modern learning systems with the power to deal with imperfect supervision. This realistic topic is referred to as weakly supervised learning (Zhou 2018).

In this paper, we focus on a critical weakly supervised learning framework called partial label learning (PLL) (Cour, Sapp, and Taskar 2011; Wu, Wang, and Zhang 2022). Specifically, PLL aims to learn a multi-class classifier from ambiguous examples where each instance is associated with a set of candidate labels, among which only one is valid. The problem of PLL naturally arises in many real-world application domains such as web mining (Luo and Orabona 2010), multimedia content analysis (Chen, Patel, and Chellappa 2017; Zeng et al. 2013), ecoinformatics (Briggs, Fern, and Raich 2012; Wang, Zhang, and Li 2022), natural language processing (Zhou et al. 2018), etc.

PLL has been extensively studied in past decades. A common thread that runs through the progress in this field is the idea of disambiguating in instances' candidate label sets. Specifically, there are two main categories of disambiguation strategies, namely identification-based disambiguation strategies and averaging-based disambiguation strategies. Identification-based strategies (Jin and Ghahramani 2002; Nguyen and Caruana 2008) treat the ground-truth label as latent variable and assume certain parametric model to estimate the confidence of each candidate label. Averaging-based strategies (Cour, Sapp, and Taskar 2011; Gong et al. 2018) treat all candidate labels equally in the training phase and yield the final predictions via modifying their modeling outputs according to different averaging strategies. In recent years, deep learning technologies have been dedicated to reinvigorating the research of PLL (Lv et al. 2020; Zhang et al. 2022; Lyu, Wu, and Feng 2022). Deep partial-label (PL) models' powerful capability of data representation helps to set new state-of-the-art performance for PLL algorithms. It has been empirically and theoretically proved that learning favourable representation could promote exploring potential association between instances and labels (Zhang, Wu, and Bao 2022; Bao, Hang, and Zhang 2021, 2022; Lv et al. 2020; Feng et al. 2020; Wen et al. 2021; Wang et al. 2022), which is beneficial to recovering the ground-truth label from candidate label set.

Recently, disentangled representation learning has re-

\*Corresponding author

Copyright © 2024, Association for the Advancement of Artificial Intelligence (www.aaai.org). All rights reserved.

ceived considerable attention (Higgins et al. 2017; Chen et al. 2017; Alemi et al. 2017). It stresses that real-world data should be typically generated from series of physically or semantically interpretable factors which are coupled with each other through a complex and heterogeneous process (Bengio, Courville, and Vincent 2013; Locatello et al. 2019b). A disentangled representation prehends information about the salient factors of variation in the data, isolating information about each specific factor in only a few (or a group of) dimensions. These explanatory factors are considered to be intrinsic properties of the entities and are of fundamental importance for distinguishing between different patterns (Peng et al. 2019; Locatello et al. 2019a; Zhang et al. 2023; Wang et al. 2023a). Commonly, in PLL, the confusing candidate labels are erroneously selected for their potential relationship with the instance in terms of certain latent factors (Xu et al. 2021; Qiao, Xu, and Geng 2023). For example, *wings* and *feathers* are two representative factors for depicting flying objects such as birds and planes. The label *plane* could be accidentally picked as a candidate label for *bird* instances due to their potential similarity in terms of the latent factor *wings*. Nonetheless, if we could explicitly disentangle the *feathers*-related information from original input data, then it will be straightforward to recognize the candidate label *plane* as a false positive label. Though intuitively learning disentangled representation is expected to facilitate label disambiguation for PL examples, few existing works were dedicated to addressing this issue.

In this paper, we pioneer the research of disentangled partial label learning and propose a novel partial label learning algorithm named TERIAL, i.e. *disenTanglEd paRtIal lAbel Learning*, which makes predictions according to derived disentangled representation of instances and label embeddings. In order to make full use of the topological information of input data, an undirected bipartite graph is constructed with PL examples, where edges only exist between the instances and their candidate labels. Based on the above data structure, TERIAL implements a tailored neighborhood routing mechanism to simultaneously infer the explanatory factors that cause the edge between adjacent nodes and augment the representation of the central node with factor-aware embedding information from related neighbors via iteratively analyzing the promising subspace clusters formed by the node and its neighbors. The estimated labeling confidence matrix is also introduced to help evaluate the contribution of each factor to the links and updated in every epoch to accommodate unreliable links owing to the inherent ambiguity of PLL. We theoretically prove that the neighborhood routing mechanism will converge to the point estimate that maximizes the marginal likelihood of observed PL training examples. Moreover, statistical distance correlation is employed to encourage independence between representation related with different latent explanatory factors. Comprehensive experiments over benchmark as well as real-world PL datasets validate the superiority of our proposed approach.

The rest of this paper is organized as follows. Section 2 briefly reviews related works on PLL and disentangled representation learning. Section 3 presents technical details of the proposed TERIAL approach. Section 4 reports experi-

mental results over a broad range of PL datasets. Finally, section 5 concludes this paper.

## Related Works

### Partial Label Learning

As an emerging weakly-supervised learning framework, partial label learning considers inaccurate supervision where each training example is associated with multiple candidate labels among which only one corresponds to the ground-truth label (Cour, Sapp, and Taskar 2011; Wu, Wang, and Zhang 2022). Disambiguating in label space is a prevalent approach to reveal concealed labeling information for PLL. Generally, disambiguation strategies can be divided into two categories, namely identification-based strategies and averaging-based strategies. For identification-based strategies, the unknown ground-truth label is treated as latent variable whose value is estimated by the assumed parametric model which is optimized with an iterative procedure (Jin and Ghahramani 2002; Liu and Dietterich 2012; Lv et al. 2020; Chai, Tsang, and Chen 2020). For averaging-based strategies, all candidate labels of PL training examples are treated equally in the training phase while the modeling outputs are averaged with proper schemes to yield the final predictions (Cour, Sapp, and Taskar 2011; Tang and Zhang 2017; Gong et al. 2018; Zhang and Yu 2015). In recent years, efficient deep neural networks compatible with stochastic optimizers have been introduced into PLL framework to handle large-scale datasets. (Lv et al. 2020; Feng et al. 2020; Wen et al. 2021) theoretically analyse the consistency and convergency of the proposed minimal loss. (Xu et al. 2021; Qiao, Xu, and Geng 2023) make the first attempt towards instance-dependent PLL and apply probabilistic models to iteratively recover label distribution for each instance. Besides, some sophisticated techniques are borrowed from other domains to improve the generalization ability of PL learning systems, such as class activation map (Zhang et al. 2022), contrastive learning (Wang et al. 2022) and graph matching (Lyu, Wu, and Feng 2022).

Despite the progress that has been made in the study of PLL, existing learning algorithms could only perceive coarse-grained correlation between instances and labels from abstract entangled representation. In this paper, we first attempt to learn disentangled representation from PL training examples to unearth the correlation at the finer granularity of latent semantic factors, which facilitate efficient discrimination between the ground-truth label and false positive labels.

### Disentangled Representation Learning

The purpose of disentangled representation learning is to identify the explanatory factors of variations behind the data (Bengio, Courville, and Vincent 2013; Locatello et al. 2019b). Specifically, the learned representation are expected to isolate information about each specific factor in only a few (or a group of) dimensions. Benefiting from separating out the underlying structure of the data into disjoint parts, disentangled representation is inherently more interpretable, robust to adversarial attack and capable of enhancing the gen-

eralization ability of learning systems (Wang et al. 2023b; Steenkiste et al. 2019; Reddy, Godfrey, and Balasubramanian 2022; Ma et al. 2019).

Disentangled representation learning has been widely studied in past years. (Kingma and Welling 2014) employs bayesian posterior inference and variational estimation to learn the latent generative factors of observed data. (Higgins et al. 2017) improves the disentangling performance by setting a weight  $\beta$  to aggressively penalize the KL divergence term in the variational auto-encoder. Moreover, some works further explore the roles of the information bottleneck term (Luo et al. 2019; Wu et al. 2020) and the total correlation term (Chen et al. 2018; Kim and Mnih 2018) respectively to refine the objective function of likelihood. Disentangled representation learning has been successfully applied in computer vision tasks (Higgins et al. 2017; Gidaris, Singh, and Komodakis 2018; Ma et al. 2018). In addition, the progress of learning disentangled representation on relational data, such as graph-structured data, has also been made in recent years (Wang et al. 2020; Zhang et al. 2020).

Nevertheless, the task of learning disentangled representation from PL examples to facilitate inducing ameliorative multi-class classifier is still a virgin problem where few efforts have been devoted. In this paper, we pioneer the research of disentangled partial label learning. The proposed approach TERIAL is detailed in the following section.

## The Proposed TERIAL Approach

### Preliminaries

**Partial Label Learning.** Let  $\mathcal{X} = \mathbb{R}^d$  denote the  $d$ -dimensional input space and  $\mathcal{Y} = \{l_1, l_2, \dots, l_q\}$  denote the label space with  $q$  class labels. Given the PL training set  $\mathcal{D} = \{(\mathbf{x}_i, S_i) | 1 \leq i \leq n\}$ , where  $\mathbf{x}_i \in \mathcal{X}$  is a  $d$ -dimensional feature vector  $[x_{i_1}, x_{i_2}, \dots, x_{i_d}]^\top$  and  $S_i \subseteq \mathcal{Y}$  is the candidate label set associated with  $\mathbf{x}_i$  among which only one is the ground-truth label, PLL aims to derive a multi-class classifier  $h : \mathcal{X} \rightarrow \mathcal{Y}$  from the training set  $\mathcal{D}$ . In this paper, TERIAL is fulfilled with the labeling confidence matrix  $\mathbf{Y} = [\mathbf{Y}(i, j)]_{n \times q}$  where each element  $\mathbf{Y}(i, j)$  represents the estimated confidence of  $l_j$  being the ground-truth label for  $\mathbf{x}_i$ . The matrix is initialized as Eq.(1) and the constraints  $\sum_{j=1}^q \mathbf{Y}(i, j) = 1 (1 \leq i \leq n)$  always hold during the learning process.

$$\forall 1 \leq i \leq n, 1 \leq j \leq q : \mathbf{Y}(i, j) = \begin{cases} \frac{1}{|S_i|}, & \text{if } l_j \in S_i \\ 0, & \text{otherwise} \end{cases} \quad (1)$$

**Disentangled Representation Learning.** Disentangled representation learning aims to identify the explanatory factors of variations behind the data and isolate information about each specific factor in only a few dimensions. Assuming that there are  $K$  latent factors to be disentangled, for an input feature vector  $\mathbf{x}_i$ , its learned disentangled representation is formulated as  $\mathbf{o}_i = [\mathbf{o}_{i_1}^\top, \dots, \mathbf{o}_{i_K}^\top]^\top \in \mathbb{R}^{K \cdot \Delta d}$ , where the  $k$ th chunked representation  $\mathbf{o}_{i_k} \in \mathbb{R}^{\Delta d}$  is for describing the aspect that is pertinent to factor  $k$ . Benefiting from explicitly characterizing the intrinsic properties of entities, learn-

ing disentangled representation is capable of enhancing the generalization ability of learning systems.

**Overview.** To deal with the PLL problem, the proposed TERIAL approach makes prediction about the category to which an instance belongs by computing the inner product between derived disentangled representation of the instance and label embeddings. In the training phase, PL examples are stored in an undirected bipartite graph to rigorously model the correlation between instances and labels, where the edge only exists between an instance and its candidate labels. The representation of instance nodes are derived from factor-specific mapping functions and the representation of label nodes are instantiated with learnable label embeddings. The constructed relational graph is then fed into the pipeline of stacked disentangling layers, which derive the disentangled representation of nodes in the graph via implementing a tailored neighborhood routing mechanism. In PLL, candidate labels are typically erroneously selected for their potential relationship with the instance in terms of certain latent factors. Accordingly, the proposed routing mechanism progressively infers the latent explanatory factors that cause the link between adjacent nodes and augments the representation of the central node with factor-aware information from specific neighbors simultaneously via iteratively analyzing the promising subspace clusters formed by the node and its neighbors. In this process, the estimated labeling confidences are introduced to help evaluate the contribution of each factor to the links and updated in every epoch to accommodate unreliable links owing to the inherent ambiguity of PLL. Finally predictions are made based on the inner product operation and the classification errors are backpropagated, allowing the mapping functions to better perceive and speculate factor-specific representation of instances. The label embeddings are also encoded to accurately capture each label's own discriminative properties in a disentangled form. As a result, the predictions of unseen instances are made barely relying on the obtained mapping functions and label embeddings. The complete procedure of TERIAL is summarized in Appendix A.1.

### Bipartite Graph Construction

Towards fully leveraging the structural information to rigorously model correlation between instances and labels, PL training examples are formulated as an undirected bipartite graph  $G = (V, E)$ , where the set of nodes  $V$  is composed of a set of instance nodes  $V_x$  and a set of label nodes  $V_y$ , i.e.,  $V = V_x \cup V_y$ ,  $|V| = n + q$ , and  $E$  denotes the set of edges. If label  $l_v$  is a candidate label of instance  $\mathbf{x}_u$ , then there will exist an edge  $e_{uv} \in E$  between node  $u$  and node  $v$ .

Assuming that there are  $K$  latent factors to be disentangled, then  $K$  mapping functions are employed to extract factor-specific feature information from instances. Particularly, the instance  $\mathbf{x}_i (1 \leq i \leq n)$  is projected into  $K$  different subspaces according to Eq.(2):

$$\mathbf{z}_{i_k} = \frac{f_k(\mathbf{x}_i)}{\|f_k(\mathbf{x}_i)\|_2} \in \mathbb{R}^{\Delta d}, 1 \leq k \leq K, \quad (2)$$

where the mapping function  $f_k(\cdot)$  could be specified with different deep models and the  $l_2$  normalization is employed

here to ensure numerical stability (Skeel 1979). Then the representation of instance node  $i$  is constructed by concatenating  $K$  factor-aware chunked representation and is denoted as  $\mathbf{z}_i = [\mathbf{z}_{i,1}^\top, \dots, \mathbf{z}_{i,K}^\top]^\top \in \mathbb{R}^{K \cdot \Delta d}$ . Since labels do not have inherent feature vectors, the representation of label nodes are similarly instantiated by embeddings with learnable parameters  $\mathbf{y}_j = [\mathbf{y}_{j,1}^\top, \dots, \mathbf{y}_{j,K}^\top]^\top \in \mathbb{R}^{K \cdot \Delta d}$  ( $1 \leq j \leq q$ ).

Provided that the instance  $\mathbf{x}_i$  does contain meaningful information about the explanatory factor  $k$ , we assume that  $\mathbf{z}_{i,k}$  approximately characterizes the  $k$ th aspect of node  $i$ . Nonetheless,  $\mathbf{z}_i$  could not be straightforwardly employed to serve as  $\mathbf{o}_i$  since the raw input data is typically insufficient to completely depict an entity in the real world (Bengio, Courville, and Vincent 2013; Locatello et al. 2019b). Accordingly, considering the prospective correlation between the instance and its candidate labels, TERIAL takes advantage of comprehensive information propagated from neighboring nodes to augment the preliminary representation  $\mathbf{z}_u$  of the central node  $u$ . The constructed graph-structure data are then fed into a pipeline consisting of stacked disentangling layers, which progressively enrich the node representation through a tailored neighborhood routing mechanism.

## The Neighborhood Routing Mechanism

The disentangling layer is deployed to yield rich and accurate disentangled representation of instances. It augments the fed nodes' representation through a tailored neighborhood routing mechanism  $g(\cdot)$ . Let  $\mathbf{w}_u$  denote the input representation of node  $u$  ( $u \in V$ ) for a disentangling layer. Next we will elaborate how the proposed routing mechanism derives the enriched representation  $\mathbf{c}_u = g(\mathbf{w}_u, \{\mathbf{w}_v | v \in \mathcal{N}_u\})$ , where  $\mathcal{N}_u$  denotes the set of neighboring nodes of node  $u$ . Without loss of generality, we will focus on the message-passing process which takes the instance node as the center. The refined representation of label nodes could be achieved in the same manner.

For the central (instance) node  $u$  ( $u \in V_x$ ), its links with candidate label nodes could be attributed to their potential relationship associated with certain explanatory factors. Moreover, owing to the inherent ambiguity of PLL, there could exist unreliable edges in the graph, i.e., the degree of correlation between one node and its neighbors could vary a lot. As a result, the proposed routing mechanism is required to simultaneously identify the true latent explanatory factors that cause the link between adjacent nodes and accurately quantify the bonds between the central node and its neighbors.

The first-order and the second-order proximity are widely accepted explanations for the existence of a link in the graph (Granovetter 1973). They are also the essential ingredients of many graph-based algorithms (Wu et al. 2020; Wang et al. 2020). Based on them, we propose two rational hypotheses, which are the foundations of the induced neighborhood routing mechanism.

**Hypothesis 1.** If a large subset of neighbors of node  $u$  have similar representation w.r.t the latent factor  $k$ , i.e., they form a cluster in the  $k$ th subspace, then factor  $k$  is likely to be a clue to the connections between node  $u$  and these neighboring nodes.

**Hypothesis 2.** If the representation of node  $u$  is similar to that of its neighboring node  $v$  in terms of aspect  $k$ , then the latent factor  $k$  is likely to be the reason why the two nodes are connected.

To propagate factor-specific information from neighbors to the central node, Hypothesis 1 inspires us to search for the largest cluster in each of the  $K$  projected subspaces. Since the central node  $u$  is not involved in the clustering procedure, Hypothesis 1 is robust under the scenario where  $\mathbf{w}_u$  is noisy or incomplete. In addition, when performing clustering in the  $k$ th subspace, irrelevant neighboring nodes will be automatically pruned, because their projected representation could be noises and will not form a large enough cluster. Though the clustering procedure is usually time-consuming due to the requirement of extensive iterations for convergence, Hypothesis 2 indicates that the value of  $\mathbf{w}_{u,k}^\top \mathbf{w}_{v,k}$  could be a hint on the factors that cause the link between nodes. Therefore, serving as a strong prior, Hypothesis 2 is adopted to guide the clustering process for faster convergence. Based on the above consideration, we introduce the proposed neighborhood routing mechanism.

Let  $p_{u,v}^k$  ( $1 \leq k \leq K$ ) quantify the influence of factor  $k$  to the link between the central node  $u$  and its neighboring node  $v$ . According to Hypothesis 2,  $p_{u,v}^k$  is initialized as:

$$p_{u,v}^{k(0)} = \frac{\exp(\frac{\mathbf{w}_{u,k}^\top \mathbf{w}_{v,k}}{\tau})}{\sum_{k'=1}^K \exp(\frac{\mathbf{w}_{u,k'}^\top \mathbf{w}_{v,k'}}{\tau})} \quad (1 \leq k \leq K), \quad (3)$$

where  $\tau$  is the smooth factor which controls the hardness of the assignment and is set as  $\tau = 1$  in this paper.

Inspired by Hypothesis 1, we then iteratively search for the largest cluster in  $K$  subspaces. Reasonably, the augmented representation of the central node  $u$  is set to be the clustering center of its neighborhoods, and the routing mechanism is formulated as follows:

$$\mathbf{c}_{u,k}^{(t)} = \frac{\mathbf{w}_{u,k} + \sum_{v \in \mathcal{N}_u} p_{u,v}^{k(t-1)} \mathbf{w}_{v,k}}{\|\mathbf{w}_{u,k} + \sum_{v \in \mathcal{N}_u} p_{u,v}^{k(t-1)} \mathbf{w}_{v,k}\|_2}, \quad (4)$$

where  $\mathbf{c}_{u,k}^{(t)}$  denotes the temporary clustering center corresponding to the  $k$ th subspace in the  $t$ th iteration. Furthermore, in order to alleviate the detrimental effect of unreliable links corresponding to false positive candidate labels in the graph, estimated labeling confidences are introduced to help update the correlation coefficient  $p_{u,v}^{k(t)}$  in each iteration:

$$p_{u,v}^{k(t)} = \mathbf{Y}(u, v) \frac{\exp(\frac{\mathbf{c}_{u,k}^{(t)\top} \mathbf{w}_{v,k}}{\tau})}{\sum_{k'=1}^K \exp(\frac{\mathbf{c}_{u,k'}^{(t)\top} \mathbf{w}_{v,k'}}{\tau})} \quad (1 \leq k \leq K). \quad (5)$$

The clustering center and correlation coefficients are iteratively updated in an alternative manner. After  $T$  iterations<sup>1</sup>, we finally obtain the constructed clustering center  $\mathbf{c}_{u,k}^{(T)}$  in each subspace and the derived representation of

<sup>1</sup>In this paper, the maximum number of iterations is set to be  $T = 6$ , which suffices to yield stable performance for the proposed approach

central node  $u$  is set as  $\mathbf{c}_u = g(\mathbf{w}_u, \{\mathbf{w}_v | v \in \mathcal{N}_u\}) = [\mathbf{c}_{u_1}^{(T)\top}, \dots, \mathbf{c}_{u_K}^{(T)\top}]^\top$ .

**Theoretical Analysis.** We theoretically analyze the convergence property of the proposed neighborhood routing mechanism and deduce the following Theorem 1. Its proof is provided in Appendix A.2.

*Theorem 1: For the vMF mixture model, the proposed neighborhood routing mechanism could be interpreted from the expectation-maximization perspective. Particularly, it converges to a point estimate of  $\{\mathbf{c}_{u_k}\}_{k=1}^K$  that maximizes the marginal likelihood  $p(\{\mathbf{w}_{i_k} : i \in \{u\} \cup \mathcal{N}_u, 1 \leq k \leq K\}; \{\mathbf{c}_{u_k}\}_{k=1}^K)$ .*

**Multi-Layer Stacking.** Above we elaborate how to utilize the proposed routing mechanism to aggregate factor-specific embedding information in the disentangling layer. Furthermore, we argue that it is feasible to stack  $L$  disentangling layers to explore rich semantics from multi-hop neighbors when producing a node's representation. Specifically, let  $\mathbf{w}_u^{(\beta)}$  and  $\mathbf{o}_u^{(\beta)}$  respectively denote the input and output representation of node  $u$  for the  $\beta$ th disentangling layer, where  $u \in V$  and  $\beta \in \{1, \dots, L\}$ . We demand that  $\mathbf{w}_u^{(\beta)} = \mathbf{o}_u^{(\beta-1)}$  ( $\beta \in \{2, \dots, L\}$ ) among multiple layers.<sup>2</sup> In order to avoid the over-smoothing issue, which is a common problem in graph learning (Chen et al. 2020), the nodes' representation in each layer are progressively assigned according to Eq.(6):

$$\mathbf{o}_u^{(\beta)} = \alpha \cdot \mathbf{w}_u^{(\beta)} + (1 - \alpha) \cdot g(\mathbf{w}_u^{(\beta)}, \{\mathbf{w}_v^{(\beta)} | v \in \mathcal{N}_u\}), \quad (6)$$

where the balancing factor is set as  $\alpha = 0.6$  in this paper.

## Independence Modeling

Though the proposed routing mechanism encourages representation conditioned on different explanatory factors to be different from each other, there still might exist redundancy among them. Accordingly, we employ the distance correlation (Székely, Rizzo, and Bakirov 2007; Wang et al. 2020) as a regularizer to encourage representation associated with different latent factors to be independent. Specifically, distance correlation is a statistical measure that is capable of characterizing independence of any two paired vectors, from their both linear and nonlinear relationships. The derived loss function is formulated as:

$$\mathcal{L}_{\text{ind}} = \sum_{k=1}^K \sum_{k'=k+1}^K \text{dCor}(\mathbf{E}_k, \mathbf{E}_{k'}), \quad (7)$$

where  $\mathbf{E}_k = [\mathbf{o}_{1_k}^{(L)\top}; \dots; \mathbf{o}_{n_k}^{(L)\top}; \mathbf{o}_{(n+1)_k}^{(L)\top}; \dots; \mathbf{o}_{(n+q)_k}^{(L)\top}] \in \mathbb{R}^{(n+q) \times \Delta^d}$ . The function of distance correlation  $\text{dCor}(\cdot, \cdot)$  is defined as:

$$\text{dCor}(\mathbf{E}_k, \mathbf{E}_{k'}) = \frac{\text{dCov}(\mathbf{E}_k, \mathbf{E}_{k'})}{\sqrt{\text{dVar}(\mathbf{E}_k) \cdot \text{dVar}(\mathbf{E}_{k'})}}, \quad (8)$$

where  $\text{dCov}(\cdot, \cdot)$  denotes the distance covariance between two matrices and  $\text{dVar}(\cdot)$  denotes the distance variance of the matrix. We refer readers to (Székely, Rizzo, and Bakirov 2007) for the details of calculation.

<sup>2</sup>For the first disentangling layer,  $\mathbf{w}_i^{(1)} = \mathbf{z}_i (1 \leq i \leq n)$  for instance nodes and  $\mathbf{w}_j^{(1)} = \mathbf{y}_j (1 \leq j \leq q)$  for label nodes.

## Model Optimization and Prediction

Through the processing of stacked disentangling layers, we eventually obtain the disentangled representation  $\mathbf{o}_i^{(L)} (1 \leq i \leq n)$  of instances. Besides, the label embeddings  $\mathbf{y}_j (1 \leq j \leq q)$  are also expected to be disentangled through model training. As a result, we simply use inner product  $s_{i,j} = \mathbf{o}_i^{(L)\top} \mathbf{y}_j$  as the score of  $l_j$  being the ground-truth label of  $\mathbf{x}_i$ . The classification loss is defined as:

$$\mathcal{L}_{\text{ce}} = \sum_{1 \leq i \leq n} \sum_{l_j \in S_i} \mathbf{Y}(i, j) l(s_{i,j}, l_j), \quad (9)$$

where  $l(\cdot, \cdot)$  denotes the cross-entropy loss function.

During training, the empirical losses  $\mathcal{L}_1 = \mathcal{L}_{\text{ce}}$  and  $\mathcal{L}_2 = \mathcal{L}_{\text{ce}} + \mathcal{L}_{\text{ind}}$  are optimized alternatively to prevent the training process from falling into local minimas (Goodfellow et al. 2014; Ren et al. 2015; Wang et al. 2020). The labeling confidence matrix is re-estimated at the end of each epoch according to Eq.(10):

$$\mathbf{Y}(i, j) = \begin{cases} \frac{s_{i,j}}{\sum_{l_{j'} \in S_i} s_{i,j'}}, & \text{if } l_j \in S_i \\ 0, & \text{otherwise.} \end{cases} \quad (10)$$

After training, mapping functions  $f_k (1 \leq k \leq K)$  are allowed to better perceive and speculative factor-specific information from the raw input data. The learned embeddings of label nodes are also encoded with each label's own discriminative properties in a disentangled form. In the testing phase, the disentangled representation of unseen instance  $\mathbf{x}'_i$  is derived as  $\mathbf{x}'_i^{\text{out}} = [f_1(\mathbf{x}'_i)^\top, \dots, f_K(\mathbf{x}'_i)^\top]^\top$  and its score about label  $l_j$  is set as  $s'_{i,j} = \mathbf{x}'_i^{\text{out}\top} \cdot \mathbf{y}_j$ . The final prediction is made by  $l^* = \arg \max_{l_j \in \mathcal{Y}} s'_{i,j}$ .

## Experiments

In this section, comprehensive experiments are conducted to verify the effectiveness of our proposed TERIAL approach.

## Classification Performance

**Datasets.** Five popular benchmark datasets are employed to generate synthetic PL data sets, including MNIST (Le-Cun et al. 1998), Kuzushiji-MNIST (abbreviated as KM-NIST) (Clanuwat et al. 2018), Fashion-MNIST (abbreviated as FMNIST) (Xiao, Rasul, and Vollgraf 2017), SVHN (Netzer et al. 2011) and CIFAR-10 (Krizhevsky, Hinton et al. 2009). More details about these benchmark datasets are shown in Appendix B.1. Following the conventional experimental protocol in PLL (Hüllermeier and Beringer 2006; Cour, Sapp, and Taskar 2011; Gong et al. 2018; Liu and Dieterich 2012), the benchmark datasets are corrupted to PL datasets with the parameter  $r$ . Specifically, for each instance,  $r$  false positive class labels are randomly selected to construct the candidate label set along with the ground-truth label. In this subsection, the number of false positive class labels is set as  $r \in \{3, 5, 7\}$ . Moreover, instance-dependent PL datasets (Qiao, Xu, and Geng 2023; Wu, Wang, and Zhang 2022) are also generated according to the same strategy utilized in (Xu et al. 2021), which made the first attempt towards instance-dependent PLL.

Datasets	Method	$r = 3$	$r = 5$	$r = 7$
MNIST	Ours	<b>98.10±0.12%</b> <b>97.71±0.09%</b> <b>96.57±0.06%</b>		
	PRODEN	97.85±0.03%	97.39±0.13%	95.77±0.24%
	RC	97.97±0.16%	97.49±0.17%	96.19±0.19%
	CC	97.80±0.12%	97.43±0.19%	96.03±0.15%
	LW	97.26±0.09%	97.19±0.22%	95.34±0.20%
	VALEN	96.54±0.19%	96.21±0.27%	94.72±0.26%
KMNIST	CAVL	97.79±0.08%	96.69±0.12%	95.52±0.16%
	Ours	<b>89.24±0.11%</b> <b>87.53±0.19%</b> <b>82.97±0.16%</b>		
	PRODEN	88.52±0.03%	85.91±0.11%	76.32±0.14%
	RC	88.78±0.07%	86.98±0.11%	80.55±0.13%
	CC	88.48±0.05%	86.84±0.17%	79.89±0.10%
	LW	87.82±0.09%	84.66±0.22%	78.41±0.19%
FMNIST	VALEN	86.71±0.23%	80.79±0.35%	73.26±0.38%
	CAVL	87.14±0.16%	82.64±0.26%	77.63±0.28%
	Ours	<b>88.68±0.08%</b> <b>87.95±0.09%</b> <b>86.69±0.05%</b>		
	PRODEN	87.51±0.11%	86.28±0.19%	84.81±0.14%
	RC	88.17±0.10%	87.42±0.16%	86.02±0.23%
	CC	87.89±0.23%	87.23±0.13%	85.87±0.12%
SVHN	LW	87.93±0.04%	86.34±0.08%	84.57±0.13%
	VALEN	83.24±0.12%	80.21±0.13%	83.86±0.22%
	CAVL	88.11±0.08%	87.48±0.10%	83.86±0.16%
	Ours	<b>95.24±0.09%</b> <b>94.77±0.12%</b> <b>93.92±0.07%</b>		
	PRODEN	94.54±0.17%	94.12±0.21%	92.78±0.26%
	RC	94.76±0.12%	94.25±0.11%	92.92±0.16%
CIFAR-10	CC	94.52±0.12%	93.83±0.11%	92.61±0.16%
	LW	94.44±0.28%	94.19±0.09%	92.66±0.14%
	VALEN	88.93±0.25%	85.36±0.28%	80.86±0.17%
	CAVL	72.05±0.13%	49.96±0.19%	35.65±0.26%
	Ours	<b>79.01±0.23%</b> <b>76.61±0.25%</b> <b>65.07±0.37%</b>		
	PRODEN	78.87±0.29%	75.59±0.34%	<b>72.34±0.46%</b>

Table 1: Classification accuracy (mean±std) of each comparing algorithm on corrupted benchmark datasets (# false positive labels  $r \in \{3, 5, 7\}$ ). The best results among methods are highlighted in bold.

We also conduct comparative experiments on real-world PL datasets. The details and empirical results are reported in Appendix C.

**Comparing Methods.** To verify the effectiveness of our proposed approach, TERIAL is compared with six state-of-the-art PLL approaches including PRODEN (Lv et al. 2020), RC, CC (Feng et al. 2020), LW (Wen et al. 2021), VALEN (Xu et al. 2021), CAVL (Zhang et al. 2022). More details about comparing algorithms are shown in Appendix B.2. Their hyper-parameters are specified according to the suggested parameter settings or searched to maximize the accuracy on a validation set containing 10% of the training samples. For TERIAL, the assumed number of latent factors is set as  $K = 10$  on datasets of MNIST, KMNIST, FMNIST and  $K = 8$  on SVHN and CIFAR-10. The number of disentangling layers is set as  $L = 2$ , which is sufficient to achieve state-of-the-art performance for our proposed approach. We use different backbones according to the target datasets. To be more specific, we employ the base model as

TERIAL- $L$	TERIAL-0	TERIAL-1	TERIAL-2	TERIAL-3
MNIST( $r = 3$ )	97.73%	97.91%	98.10%	98.13%
SVHN( $r = 7$ )	92.67%	93.33%	93.92%	93.96%

Table 2: Impact of the number of disentangling layers  $L \in \{0, 1, 2, 3\}$  on the classification performance of TERIAL on datasets MNIST( $r = 3$ ) and SVHN( $r = 7$ ).

TERIAL(varying $K$ )	$K = 1$	$K = 5$	$K = 10$	$K = 20$	$K = 25$
KMNIST( $r = 5$ )	86.14%	86.62%	87.53%	86.92%	86.67%
FMNIST( $r = 5$ )	86.11%	86.82%	87.95%	88.13%	88.05%

Table 3: Impact of the assumed number of latent explanatory factors  $K$  on the classification performance of TERIAL on datasets of KMNIST( $r = 5$ ) and FMNIST( $r = 5$ ).

a 3-layer MLP ( $d = 300 - 100 - 10$ ) on MNIST, KMNIST, FMNIST and a 34-layer ResNet on SVHN and CIFAR-10. For the fairness of comparison, the mapping function  $f_k(\cdot)$  of TERIAL is set as the base model removing the classification layer. For all DNN based methods, we search the initial learning rate from  $\{10^{-1}, 10^{-2}, 10^{-3}, 10^{-4}\}$  and the weight decay from  $\{10^{-2}, 10^{-3}, 10^{-4}, 10^{-5}\}$ . The mini-batch size is set as 256 and the number of epochs is set as 200. All the models are trained with stochastic gradient descent (SGD) (Robbins and Monro 1951) optimizer with momentum 0.9. All experiments are repeated for 5 times with different random seeds, and the average accuracy and the standard deviation are reported.

**Empirical Results.** The predictive performance (mean±std) of comparing algorithms on benchmark datasets corrupted by  $r \in \{3, 5, 7\}$  are reported in Table 1, where the best results are highlighted in bold. In addition, the corresponding results of pairwise  $t$ -test at 0.05 significance level are reported in Appendix B.3. Out of the 90 statistical comparisons (6 comparing algorithms  $\times$  5 datasets  $\times$  3 settings of  $r$ ), TERIAL outperforms all other state-of-the-art algorithms in 86 cases, with only two losses of comparisons against PRODEN and RC on CIFAR-10. These impressive results suggest that the learned disentangled representation from PL examples could more accurately and profoundly characterize the essential properties of instances thus helping the classifier to disambiguate and predict.

In addition, the predictive performance (mean±std) of comparing algorithms on instance-dependent benchmark datasets, are reported in Appendix B.4. We observe that TERIAL could still achieve best results in most cases, with the only exception on CIFAR-10 against PRODEN and RC. This indicates that the disentangled representation could better clarify the dependency between instances and labels.

## Further Studies

In this section, we investigate the rationality and effectiveness of some designs of our TERIAL approach.

**Impact of Disentangling Layers.** The disentangling layers implemented by proposed neighborhood routing mechanism are the core of TERIAL. Here we investigate how the number of such layers  $L \in \{0, 1, 2, 3\}$  affects the model’s classifi-

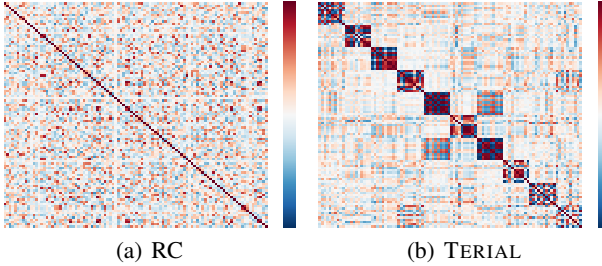


Figure 1: The values of the correlation between the elements of the 100-dimensional representation learned by RC and TERIAL with 10 assumed latent factors on the test dataset of KMNIST( $r = 5$ ).

cation performance. The TERIAL approach with  $L$  disentangling layers is denoted as TERIAL- $L$  and the corresponding results on corrupted datasets of MNIST( $r = 3$ ) and SVHN( $r = 7$ ) are summarized in Table 2. We can observe that the neighborhood routing mechanism really helps capture sophisticated and complete disentangling information since TERIAL-0 is inferior to all of other compared approaches. Moreover, we find that gather information from multi-hop neighbors could lead to better performance though the margin could be small (between TERIAL-2 and TERIAL-3) as  $L$  gets larger. As a result, in this paper we set  $L = 2$  and further improvement is expected to be achieved through fine-tuning  $L$ .

For TERIAL,  $K$  is an important hyper-parameter which decides the assumed number of latent explanatory factors. Accordingly, we investigate how the predictive performance varies with the parameter  $K$  on the corrupted datasets of KMNIST( $r = 5$ ) and FMNIST( $r = 5$ ). As is shown in Table 3, the performance corresponding to  $K = 1$  is inferior to all other comparing results. This suggests that learned abstract entangled representation is of limited help to the learning system in distinguishing between different categories. Moreover, we find that increasing  $K$  from 1 to 10 could absolutely enhance the model’s classification performance. This strongly justifies that disentangled representation could facilitate disambiguation for PL examples. However, the classification accuracy drops when  $K$  gets larger. It’s likely that as  $K$  increases, the dimensionality of chunked representation  $\Delta d = \frac{d'}{K}$  becomes smaller and thus the disentangled components gradually lose their ability to completely portray the explanatory factors of instances.<sup>3</sup>

In addition, the learning rate  $\alpha$  and the maximum number of iterations  $T$  are key hyper-parameters for the routing mechanism. The ablation studies on these two parameters are provided in Appendix D.1.

**Impact of Independence Modeling.** In the independence modeling module, the statistical distance correlation is applied to encourage independence between factor-specific chunked representation. The derived loss function  $\mathcal{L}_{\text{ind}}$  are optimized alternatively to prevent the training process

<sup>3</sup>Here  $d' = 100$ , which is the number of neurons in the second hidden layer of the base model.

from falling into local minimas. We evaluate the performance of TERIAL with(w/ or without(w/o) the independence modeling module on benchmark datasets corrupted by the instance-dependent strategy, and the results are reported in Appendix D.2. We can observe that in all five benchmark datasets removing independence modeling module will lead to performance drop.

## Visualization

In this part, we visualize the disentangled representation learned by TERIAL from multiple perspectives. The corresponding results of the best baseline RC that is theoretically proved risk-consistent are also reported for comparison.<sup>4</sup>

Firstly, in Fig. 1, values of correlation between the elements of the 100-dimensional representation learned by RC and TERIAL with 10 latent factors on the test dataset of KMNIST( $r = 5$ ) are presented in a heat-map. The heat-map for TERIAL exhibits ten clear diagonal blocks while there are not obvious correlation between features learned by RC. This indicates that disentangled representation learned by TERIAL could definitely capture mutually exclusive information associated with different explanatory factors.

In addition, we visualize the representation produced by TERIAL and RC on the test dataset of SVHN( $r = 5$ ) in Appendix E. We can observe that in the t-SNE (Van der Maaten and Hinton 2008) visualization where representation are produced by RC, the class boundaries are not clear while some classes overlap. On the contrary, representation produced by TERIAL are more distinguishable and lead to well-separated clusters. This suggests that TERIAL could capture high-quality representation from PL examples through disentangled representation learning, thus improving the generalization ability of the learned classifier.

## Conclusion

In this paper, we make the first attempt towards disentangled partial label learning. A novel PLL approach named TERIAL is proposed, which makes predictions based on derived disentangled representation of instances and label embeddings. Specifically, in TERIAL, the partial label examples are stored in an undirected bipartite graph to rigorously model the correlation between instances and labels. Then TERIAL employs a tailored neighborhood routing mechanism to progressively infer the explanatory factors that cause the edge between adjacent nodes and augment the representation of the central node by propagating proper disentangling information from related neighbors. The estimated labeling confidence matrix is also introduced to accommodate unreliable links due to the inherent ambiguity of PLL. In addition, the statistical distance correlation is employed to encourage the independence between representation corresponding to different latent factors. Extensive experiments over various datasets verify the effectiveness of our proposed approach.

<sup>4</sup>The representation provided by TERIAL denotes the output of mapping functions and the representation provided by RC denotes the output of the base model removing the classification layer.

## Acknowledgements

The authors wish to thank the anonymous reviewers for their helpful comments and suggestions. This work was supported by the National Science Foundation of China (62225602), and the Big Data Computing Center of Southeast University.

## References

Alemi, A. A.; Fischer, I.; Dillon, J. V.; and Murphy, K. 2017. Deep variational information bottleneck. In *Proceedings of the 5th International Conference on Learning Representations*. Toulon, France.

Bao, W.-X.; Hang, J.-Y.; and Zhang, M.-L. 2021. Partial label dimensionality reduction via confidence-based dependence maximization. In *Proceedings of the 27th ACM SIGKDD Conference on Knowledge Discovery and Data Mining*, 46–54. Virtual Event.

Bao, W.-X.; Hang, J.-Y.; and Zhang, M.-L. 2022. Submodular feature selection for partial label learning. In *Proceedings of the 28th ACM SIGKDD Conference on Knowledge Discovery and Data Mining*, 26–34. Washington D.C.

Bengio, Y.; Courville, A.; and Vincent, P. 2013. Representation learning: A review and new perspectives. *IEEE Transactions on Pattern Analysis and Machine Intelligence*, 35(8): 1798–1828.

Briggs, F.; Fern, X. Z.; and Raich, R. 2012. Rank-loss support instance machines for MIML instance annotation. In *Proceedings of the 18th ACM SIGKDD International Conference on Knowledge Discovery and Data Mining*, 534–542. Beijing, China.

Chai, J.; Tsang, I. W.; and Chen, W. 2020. Large margin partial label machine. *IEEE Transactions on Neural Networks and Learning Systems*, 31(7): 2594–2608.

Chen, C.-H.; Patel, V. M.; and Chellappa, R. 2017. Learning from ambiguously labeled face images. *IEEE Transactions on Pattern Analysis and Machine Intelligence*, 40(7): 1653–1667.

Chen, D.; Lin, Y.; Li, W.; Li, P.; Zhou, J.; and Sun, X. 2020. Measuring and relieving the over-smoothing problem for graph neural networks from the topological view. In *Proceedings of the 34th AAAI Conference on Artificial Intelligence*, 3438–3445. New York, NY.

Chen, T. Q.; Li, X.; Grosse, R. B.; and Duvenaud, D. 2018. Isolating sources of disentanglement in variational autoencoders. In *Advances in Neural Information Processing Systems 31*, 2615–2625. Montréal, Canada.

Chen, X.; Kingma, D. P.; Salimans, T.; Duan, Y.; Dhariwal, P.; Schulman, J.; Sutskever, I.; and Abbeel, P. 2017. Variational lossy autoencoder. In *Proceedings of the 5th International Conference on Learning Representations*. Toulon, France.

Clanuwat, T.; Bober-Irizar, M.; Kitamoto, A.; Lamb, A.; Yamamoto, K.; and Ha, D. 2018. Deep learning for classical Japanese literature. *arXiv:1812.01718*.

Cour, T.; Sapp, B.; and Taskar, B. 2011. Learning from partial labels. *Journal of Machine Learning Research*, 12: 1501–1536.

Feng, L.; Lv, J.; Han, B.; Xu, M.; Niu, G.; Geng, X.; An, B.; and Sugiyama, M. 2020. Provably consistent partial-label learning. In *Advances in Neural Information Processing Systems 33*, 6–12. Virtual Event.

Gidaris, S.; Singh, P.; and Komodakis, N. 2018. Unsupervised representation learning by predicting image rotations. In *Proceedings of the 6th International Conference on Learning Representations*. Vancouver, Canada.

Gong, C.; Liu, T.; Tang, Y.; Yang, J.; Yang, J.; and Tao, D. 2018. A regularization approach for instance-based superset label learning. *IEEE Transactions on Cybernetics*, 48(3): 967–978.

Goodfellow, I. J.; Pouget-Abadie, J.; Mirza, M.; Xu, B.; Warde-Farley, D.; Ozair, S.; Courville, A. C.; and Bengio, Y. 2014. Generative adversarial nets. In *Advances in Neural Information Processing Systems 27*, 2672–2680. Montreal, Canada.

Granovetter, M. S. 1973. The strength of weak ties. *American Journal of Sociology*, 78(6): 1360–1380.

Higgins, I.; Matthey, L.; Pal, A.; Burgess, C. P.; Glorot, X.; Botvinick, M. M.; Mohamed, S.; and Lerchner, A. 2017. beta-VAE: Learning basic visual concepts with a constrained variational framework. In *Proceedings of the 5th International Conference on Learning Representations*. Toulon, France.

Hu, H.; Yang, Y.; Yin, Y.; and Wu, J. 2022. Metric learning for domain adversarial network. *Frontiers of Computer Science*, 16(5): 165341.

Hüllermeier, E.; and Beringer, J. 2006. Learning from ambiguously labeled examples. *Intelligent Data Analysis*, 10(5): 419–439.

Jin, R.; and Ghahramani, Z. 2002. Learning with multiple labels. In *Advances in neural information processing systems 15*, 897–904. Vancouver, Canada.

Kim, H.; and Mnih, A. 2018. Disentangling by factorising. In *Proceedings of the 35th International Conference on Machine Learning*, 2654–2663. Stockholm, Sweden.

Kingma, D. P.; and Welling, M. 2014. Auto-encoding variational bayes. In *Proceedings of the 2nd International Conference on Learning Representations*. Banff, Canada.

Krizhevsky, A.; Hinton, G.; et al. 2009. Learning multiple layers of features from tiny images. *Technique Report*.

LeCun, Y.; Bengio, Y.; and Hinton, G. 2015. Deep learning. *Nature*, 521(7553): 436–444.

LeCun, Y.; Bottou, L.; Bengio, Y.; and Haffner, P. 1998. Gradient-based learning applied to document recognition. *Proceedings of the IEEE*, 86(11): 2278–2324.

Liu, L.; and Dietterich, T. 2012. A conditional multinomial mixture model for superset label learning. In *Advances in Neural Information Processing Systems 25*, 557–565. Cambridge, MA.

Locatello, F.; Abbati, G.; Rainforth, T.; Bauer, S.; Schölkopf, B.; and Bachem, O. 2019a. On the fairness of disentangled representations. In *Advances in Neural Information Processing Systems 32*, 14584–14597. Vancouver, Canada.

Locatello, F.; Bauer, S.; Lucic, M.; Rätsch, G.; Gelly, S.; Schölkopf, B.; and Bachem, O. 2019b. Challenging common assumptions in the unsupervised learning of disentangled representations. In *Proceedings of the 36th International Conference on Machine Learning*, 4114–4124. Long Beach, CA.

Luo, J.; and Orabona, F. 2010. Learning from candidate labeling sets. In *Advances in Neural Information Processing Systems 23*, 1504–1512. Cambridge, MA.

Luo, Y.; Liu, P.; Guan, T.; Yu, J.; and Yang, Y. 2019. Significance-aware information bottleneck for domain adaptive semantic segmentation. In *Proceedings of the International Conference on Computer Vision*, 6777–6786. Seoul, Korea.

Lv, J.; Xu, M.; Feng, L.; Niu, G.; Geng, X.; and Sugiyama, M. 2020. Progressive identification of true labels for partial-label learning. In *Proceedings of the 37th International Conference on Machine Learning*, 6500–6510. Virtual Event.

Lyu, G.; Wu, Y.; and Feng, S. 2022. Deep graph matching for partial label learning. In *Proceedings of the 31st International Joint Conference on Artificial Intelligence*, 3306–3312. Vienna, Austria.

Ma, J.; Cui, P.; Kuang, K.; Wang, X.; and Zhu, W. 2019. Disentangled graph convolutional networks. In *Proceedings of the 36th*

*International Conference on Machine Learning*, 4212–4221. Long Beach, CA.

Ma, L.; Sun, Q.; Georgoulis, S.; Gool, L. V.; Schiele, B.; and Fritz, M. 2018. Disentangled person image generation. In *Proceedings of the 31st IEEE Conference on Computer Vision and Pattern Recognition*, 99–108. Salt Lake, UT.

Netzer, Y.; Wang, T.; Coates, A.; Bissacco, A.; Wu, B.; and Ng, A. Y. 2011. Reading digits in natural images with unsupervised feature learning. In *Proceedings of the NIPS Workshop on Deep Learning and Unsupervised Feature Learning*.

Nguyen, N.; and Caruana, R. 2008. Classification with partial labels. In *Proceedings of the 14th ACM SIGKDD International Conference on Knowledge Discovery and Data Mining*, 551–559. Las Vegas, NV.

Peng, X.; Huang, Z.; Sun, X.; and Saenko, K. 2019. Domain agnostic learning with disentangled representations. In *Proceedings of the 36th International Conference on Machine Learning*, 5102–5112. Long Beach, CA.

Qiao, C.; Xu, N.; and Geng, X. 2023. Decomposition-based generation process for instance-dependent partial label learning. In *Proceedings of the 11th International Conference on Learning Representations*. Kigali, Rwanda.

Reddy, A. G.; Godfrey, B.; and Balasubramanian, V. N. 2022. On causally disentangled representations. In *Proceedings of the 34th AAAI Conference on Artificial Intelligence*, 8089–8097. Virtual Event.

Ren, S.; He, K.; Girshick, R. B.; and Sun, J. 2015. Faster r-cnn: Towards real-time object detection with region proposal networks. In *Advances in Neural Information Processing Systems 28*, 91–99. Montreal, Canada.

Robbins, H.; and Monro, S. 1951. A stochastic approximation method. *The Annals of Mathematical Statistics*, 400–407.

Skeel, R. D. 1979. Scaling for numerical stability in gaussian elimination. *Journal of the ACM*, 26(3): 494–526.

Steenkiste, S.-V.; Locatello, F.; Schmidhuber, J.; and Bachem, O. 2019. Are disentangled representations helpful for abstract visual reasoning? In *Advances in Neural Information Processing Systems 32*, 14222–14235. Vancouver, Canada.

Székely, G. J.; Rizzo, M. L.; and Bakirov, N. K. 2007. Measuring and testing dependence by correlation of distances. *The Annals of Statistics*, 35(6): 2769–2794.

Tang, C.-Z.; and Zhang, M.-L. 2017. Confidence-rated discriminative partial label learning. In *Proceedings of the 31st AAAI Conference on Artificial Intelligence*, 2611–2617. San Francisco, CA.

Van der Maaten, L.; and Hinton, G. 2008. Visualizing data using t-SNE. *Journal of Machine Learning Research*, 9(11): 2579–2605.

Wang, D.; Deng, Y.; Yin, Z.; Shum, H.-Y.; and Wang, B. 2023a. Progressive disentangled representation learning for fine-grained controllable talking head synthesis. In *Proceedings of the 36th IEEE Conference on Computer Vision and Pattern Recognition*, 17979–17989. Vancouver, Canada.

Wang, D.-B.; Zhang, M.-L.; and Li, L. 2022. Adaptive graph guided disambiguation for partial label learning. *IEEE Transactions on Pattern Analysis and Machine Intelligence*, 44(12): 8796–8811.

Wang, H.; Xiao, R.; Li, Y.; Feng, L.; Niu, G.; Chen, G.; and Zhao, J. 2022. PiCO: Contrastive label disambiguation for partial label learning. In *Proceedings of the 10th International Conference on Learning Representations*. Virtual Event.

Wang, X.; Chen, H.; Zhou, Y.; Ma, J.; and Zhu, W. 2023b. Disentangled representation learning for recommendation. *IEEE Transactions on Pattern Analysis and Machine Intelligence*, 45(1): 408–424.

Wang, X.; Jin, H.; Zhang, A.; He, X.; Xu, T.; and Chua, T. 2020. Disentangled graph collaborative filtering. In *Proceedings of the 43rd International ACM SIGIR Conference on Research and Development in Information Retrieval*, 1001–1010. Virtual Event.

Wei, T.; Wang, H.; Tu, W.; and Li, Y. 2022. Robust model selection for positive and unlabeled learning with constraints. *Science China Information Sciences*, 65(11): 1–13.

Wen, H.; Cui, J.; Hang, H.; Liu, J.; Wang, Y.; and Lin, Z. 2021. Leveraged weighted loss for partial label learning. In *Proceedings of the 38th International Conference on Machine Learning*, 11091–11100. Virtual Event.

Wu, D.-D.; Wang, D.-B.; and Zhang, M.-L. 2022. Revisiting consistency regularization for deep partial label learning. In *Proceedings of the 39th International Conference on Machine Learning*, 24212–24225. Baltimore, MD.

Wu, T.; Ren, H.; Li, P.; and Leskovec, J. 2020. Graph information bottleneck. In *Advances in Neural Information Processing Systems 33*, 20437–20448. Virtual Event.

Xiao, H.; Rasul, K.; and Vollgraf, R. 2017. Fashion-MNIST: A novel image dataset for benchmarking machine learning algorithms. *arXiv:1708.07747*.

Xu, N.; Qiao, C.; Geng, X.; and Zhang, M.-L. 2021. Instance-dependent partial label learning. In *Advances in Neural Information Processing Systems 34*, 27119–27130. Virtual Event.

Yang, C.; Liu, C.; and Yin, X.-C. 2022. Weakly correlated knowledge integration for few-shot image classification. *Machine Intelligence Research*, 19(1): 24–37.

Zeng, Z.; Xiao, S.; Jia, K.; Chan, T.-H.; Gao, S.; Xu, D.; and Ma, Y. 2013. Learning by associating ambiguously labeled images. In *Proceedings of the 26th IEEE Conference on Computer Vision and Pattern Recognition*, 708–715. Portland, OR.

Zhang, F.; Feng, L.; Han, B.; Liu, T.; Niu, G.; Qin, T.; and Sugiyama, M. 2022. Exploiting class activation value for partial-label learning. In *Proceedings of the 10th International Conference on Learning Representations*. Virtual Event.

Zhang, M.-L.; Wu, J.-H.; and Bao, W.-X. 2022. Disambiguation enabled linear discriminant analysis for partial label dimensionality reduction. *ACM Transactions on Knowledge Discovery from Data*, 16(4): 72:1–72:18.

Zhang, M.-L.; and Yu, F. 2015. Solving the partial label learning problem: An instance-based approach. In *Proceedings of the 24th International Joint Conference on Artificial Intelligence*, 4048–4054. Buenos Aires, Argentina.

Zhang, X.; Li, X.; Sultani, W.; Zhou, Y.; and Wshah, S. 2023. Cross-view geo-localization via learning disentangled geometric layout correspondence. In *Proceedings of the 37th AAAI Conference on Artificial Intelligence*, 3480–3488. Washington D.C.

Zhang, Y.; Zhu, Z.; He, Y.; and Caverlee, J. 2020. Content-collaborative disentanglement representation learning for enhanced recommendation. In *Proceedings of the 14th ACM Conference on Recommender Systems*, 43–52. Virtual Event.

Zhou, D.; Zhang, Z.; Zhang, M.-L.; and He, Y. 2018. Weakly supervised POS tagging without disambiguation. *ACM Transactions on Asian and Low-Resource Language Information Processing*, 17(4): 1–19.

Zhou, Z.-H. 2018. A brief introduction to weakly supervised learning. *National Science Review*, 5(1): 44–53.